

Article

Inhibition of Biofilm Formation by Modified Oxylipins from the Shipworm Symbiont *Teredinibacter turnerae*

Noel M. Lacerna II¹, Cydee Marie V. Ramones¹, Jose Miguel D. Robes¹, Myra Ruth D. Picart¹, Jortan O. Tun¹, Bailey W. Miller² , Margo G. Haygood², Eric W. Schmidt², Lilibeth A. Salvador-Reyes¹  and Gisela P. Concepcion^{1,*}

¹ The Marine Science Institute, University of the Philippines Diliman, Quezon City 1101, Philippines; noel.lacerna@utah.edu (N.M.I.II); cvramones@up.edu.ph (C.M.V.R.); miguel.robres@utah.edu (J.M.D.R.); mdpicart@upd.edu.ph (M.R.D.P.); jortan.tun@utah.edu (J.O.T.); lsreyes@msi.upd.edu.ph (L.A.S.-R.)

² Department of Medicinal Chemistry, University of Utah, Salt Lake City, UT 84112, USA; bailey.miller@utah.edu (B.W.M.); margo.haygood@utah.edu (M.G.H.); ews1@utah.edu (E.W.S.)

* Correspondence: gpconcepcion@up.edu.ph; Tel.: +632-8275-2877

Received: 23 November 2020; Accepted: 16 December 2020; Published: 20 December 2020



Abstract: The bioactivity-guided purification of the culture broth of the shipworm endosymbiont *Teredinibacter turnerae* strain 991H.S.0a.06 yielded a new fatty acid, turneroic acid (**1**), and two previously described oxylipins (**2–3**). Turneroic acid (**1**) is an 18-carbon fatty acid decorated by a hydroxy group and an epoxide ring. Compounds **1–3** inhibited bacterial biofilm formation in *Staphylococcus epidermidis*, while only **3** showed antimicrobial activity against planktonic *S. epidermidis*. Comparison of the bioactivity of **1–3** with structurally related compounds indicated the importance of the epoxide moiety for selective and potent biofilm inhibition.

Keywords: anti-biofilm; oxylipins; *Staphylococcus epidermidis*; Lyrodus; shipworm; *Teredinibacter turnerae*

1. Introduction

Microorganisms often colonize surfaces by creating a protected and nutritionally rich ecological niche called a biofilm [1]. Biofilms provide protected access to nutritional sources, facilitate cellular communication, and increase tolerance to antimicrobials in concentrations normally lethal to planktonic organisms [2,3]. *Staphylococcus epidermidis*, a normally commensal bacterium common in skin and mucous membranes that is pathogenic in certain circumstances, is considered the best-known example of a pathogen that uses biofilm formation as a virulence factor [4]. *S. epidermidis* biofilm-mediated infections represent the most common infections on indwelling medical devices, and the only effective treatment is the replacement of infected devices with new and uninfected ones [4,5]. Currently, research is focused on understanding the in-depth mechanism of biofilm formation. The use of small molecules affecting biofilm-associated infections could provide a solution to this longstanding problem.

Nature has historically been the most productive source of antibiotics [6]. In recent years, a strategy has been to search for bioactive compounds in previously overlooked habitats such as host-associated bacteria [7,8]. Shipworms (family: *Teredinidae*) are marine wood-boring bivalves that possess bacterial endosymbionts in bacteriocytes located in the gills [9,10]. The specialized intracellular bacteria support the host's nutrition by producing enzymes used to digest cellulose and fix nitrogen [11]. One of the major bacterial symbionts in shipworms is *Teredinibacter turnerae*, although several other species have also been identified. Genomic analysis of *T. turnerae* strain T7901 showed that an unusually high proportion of the genome (7%) is devoted to secondary metabolism [12], comparable to that of the biomedically important *Actinobacteria*. The substantial investment of *T. turnerae* in secondary metabolite biosynthesis

suggests a potential role for small molecules in the symbiotic relationship between *T. turnerae* and the shipworm host as well as other microorganisms. For example, the macrodiolide tartrolon antibiotics produced by *T. turnerae* T7901 were shown to inhibit other shipworm symbionts and free-living pathogenic bacteria [13]. The siderophore turnerbactins provide another mechanism for microbial competition in the host through iron sequestration [9]. However, despite the vast potential for natural product discovery highlighted by the genomic analysis, few compounds have been isolated and characterized from this interesting bacterial group.

In this study, we screened shipworm-associated microorganisms for antimicrobial and biofilm inhibitory activity. One of the bioactive isolates, *Teredinibacter turnerae* strain 991H.S.0a.06 from *Lyrodus pedicellatus*, was subjected to bioassay-guided fractionation, and gave the new compound turneroic acid (**1**), and two known fatty acids (**2–3**). Structure–activity comparison of **1–3** with related compounds provided insights into the critical pharmacophore for potent and selective biofilm inhibition.

2. Results and Discussion

2.1. Structure Elucidation

Turneroic acid (**1**) was purified as a white powder with λ_{\max} of 230 nm. HRESIMS of **1** showed a sodiated peak at m/z 337.2363, which was assigned to a molecular formula of $C_{18}H_{34}O_4Na$. The 1H NMR profile of turneroic acid (**1**) showed characteristic signals for oxylipins with a terminal methyl (δ_H 0.92), methylene envelope (δ_H 1.33–1.35), and α -methylenes (δ_H 2.24) (Table 1 and Supplementary Figure S2). COSY, HSQC, and HMBC showed distinctive signals for a carboxylic acid (δ_C 178.1), an epoxide moiety (δ_C/δ_H 63.4/2.67; 57.7/2.86), and a hydroxylated methine (δ_C/δ_H 72.8/3.30). 2D NMR correlations allowed for the assignment of three partial structures (Figure 1). After the assignment of these partial structures a methylene envelope remained, consisting of a C_5H_{10} unit in which the 1H and ^{13}C shifts were overlapping. While minor impurities were observed in the TOCSY spectrum of **1** due to prolonged storage in solution, clear correlations were observed between H-13/H-18 and H-14/H-18, and established the linkage between partial structures I and II. This was corroborated by the lack of TOCSY correlation between the terminal CH_3 (δ_H 0.92) and the hydroxylated methine (δ_H 3.30). HMBC correlations between H-2/C-4, H-9/C-8, H-9/C-7, and H-10/C-8 indicated that partial structures II and III were linked by the methylene envelope. Hence, the structure of **1** was assigned as 11-hydroxy-12,13-epoxy-octadecanoic acid. A somewhat similar compound, except with additional unsaturation, was previously synthesized, although no spectroscopic or configurational data were provided for the synthetic compound. Since the synthetic compound potentially consists of a mixture of four diastereomers as drawn, the identity of the compound is somewhat unclear [14]. A coupling constant of 2.1 Hz was observed for H-12 and H-13, indicating a *trans* configuration for the epoxide moiety (Table 1).

The 1H NMR spectra of **2** and **3** also showed characteristic signals for fatty acids (Supplementary Materials Figures S11 and S12). The 1H NMR and MS data for **2** matched the known compound (*E*)-9-oxohexadec-10-enoic acid, which was previously purified from the red alga *Gracilaria verrucosa* (Figure 2) [15]. The 1H NMR data for **3** showed marked similarity with **2**, indicating that these are analogues. HRESIMS analysis of **3** gave a 28 Da mass difference with **2**, suggesting two additional methylenes in **3**. This is in accordance with the additional methylene protons observed in the 1H NMR spectrum of **3** (Supplementary Materials Figure S12). Dereplication and further MS/MS fragmentation indicated that **3** was (*E*)-11-oxooctadec-12-enoic acid (Figure 2), previously reported from the marine green alga *Ulva fasciata* [16] (Supplementary Materials Figure S10).

Table 1. NMR spectroscopic data for turneroic acid (**1**) in CD₃OD.

C/H	δ C ^a	δ H (J in Hz) ^b	COSY ^b	TOCSY	HMBC ^b
1	178.1, C				
2	36.3, CH ₂	2.24, t (7.1)	3	3,4	1, 3, 4
3	26.4, CH ₂	1.60, m	2,4	2,4	4/5
4	30.4, CH ₂	1.33, m	^c	^c	3
5	30.4, CH ₂	1.33, m	^c	^c	
6	30.4, CH ₂	1.33, m	^c	^c	
7	30.4, CH ₂	1.33, m	^c	^c	
8	30.4, CH ₂	1.33, m	^c	^c	
9	26.5, CH ₂	1.46, m	8, 10		7/8, 11
10	35.2, CH ₂	1.53, 1.34, m	9, 11	11	8, 11
11	72.8, CH	3.30, m	10, 12	10, 12	9, 10, 12, 13(w)
12	63.4, CH	2.67, dd (6.6, 2.1)	11, 13	11	11, 13(w)
13	57.7, CH	2.86, td (5.8, 2.1)	12, 14	14, 16, 18	14
14	32.6, CH ₂	1.54, 1.35, m	13, 15	11, 12, 13, 15	12, 13
15	26.4, CH ₂	1.35, m	^c	^c	
16	32.8, CH ₂	1.45, m	17	18	
17	23.7, CH ₂	1.35, m	16, 18	18	18
18	14.3, CH ₃	0.92, t (7.1)	17	13, 14, 15, 16, 17	16, 17

^a 125 MHz, ^b 500 MHz, ^c overlapping peaks.

Compounds **1** and **3** are structurally related. Both are 18-carbon fatty acids, with structural modifications at C-11–C-13. Turneroic acid (**1**) bears an epoxide at C-12–C-13 instead of a C=C (as in **3**), and a hydroxy instead of a keto group at C-11. This likely points to turneroic acid being a biotransformation product of **3**. This is analogous to the enzymatic and non-enzymatic conversion of linoleic acid to the corresponding hydroxyepoxy-octadecenoic acid in human plasma [14]. On the basis of **1** and **3** having the same biosynthetic origin, the relative configuration of the epoxide moiety in **1** is likely to be *trans*. This also corroborates with the assigned relative configuration of **1** based on the $J_{H12-H13}$. The ¹H NMR spectrum of **3** gave a coupling constant of $J \sim 15.7$ Hz for the olefinic protons ($\delta_H = 6.12$ and 6.95), suggesting a *trans* coupling between H-12 and H-13. The configuration of turneroic acid (**1**) could not be assigned due to insufficient material. Nonetheless, the structural features inspired us to explore biological activity using simpler analogues (see below).

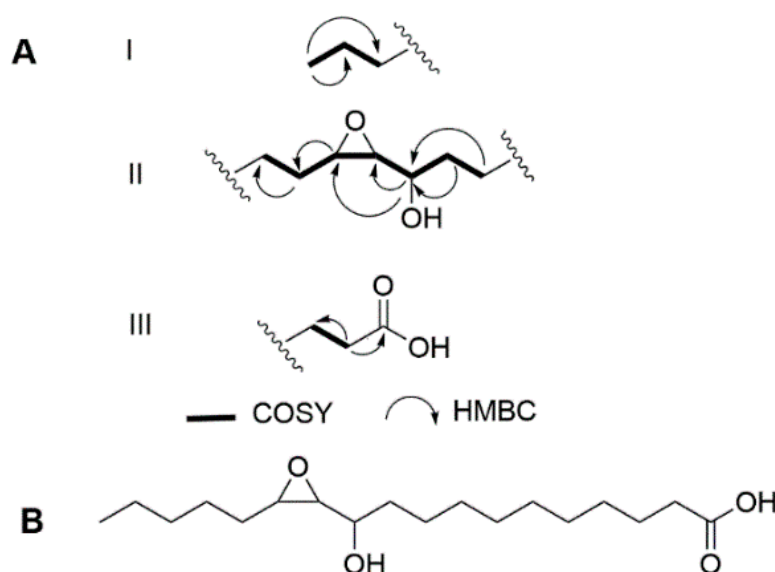


Figure 1. (A) Key fragments with COSY and HMBC correlations and (B) structure of turneroic acid (**1**).

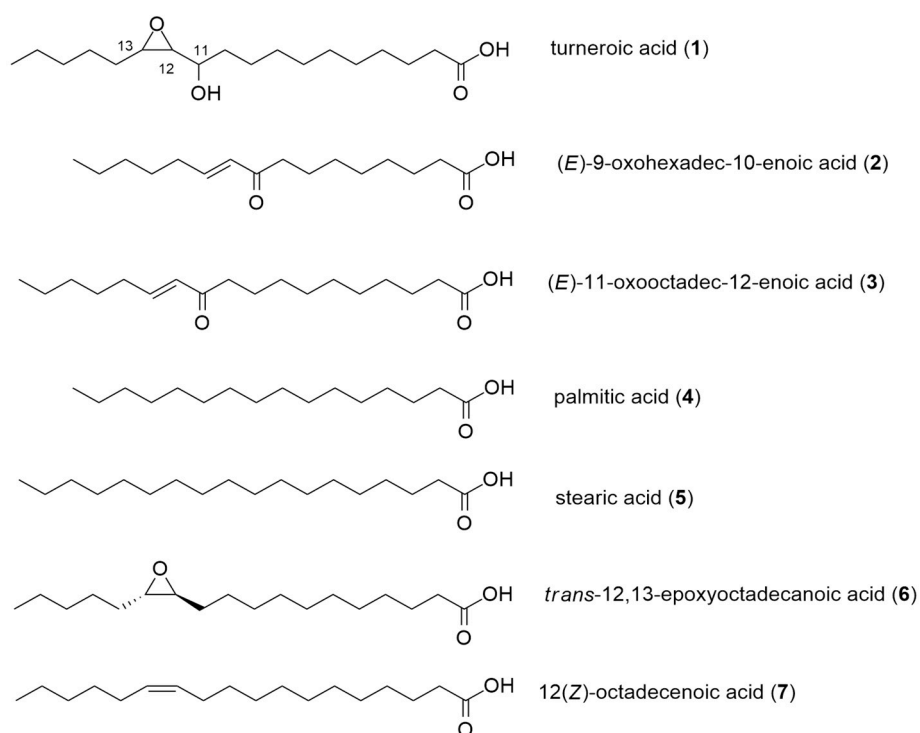


Figure 2. Structure of modified oxylipins.

2.2. Biological Activities of Oxylipins (1–7)

Compounds 1–3 are structurally related to the naturally occurring fatty acids palmitic acid (4) and stearic acid (5), as well as possible biotransformation compounds *trans*-12,13-epoxy-octadecanoic acid (6) and 12(*Z*)-octadecenoic acid (7) (Figure 2). All seven compounds were subjected to a panel of bioactivity assays to assess their effects on staphylococcal pathogens and mammalian cells (Table 2). Biofilm formation by *S. epidermidis* in the presence of 1–7 was determined by quantifying the biomass of the formed biofilm after 24 h of incubation using Alexa Fluor 488 (WGA488)-labelled wheat germ agglutinin. This fluorescent stain specifically binds to sialic acid and the N-acetylglucosaminyl residues of the biofilm. The growth of planktonic *Staphylococcus aureus*, methicillin-resistant *S. aureus*, and *S. epidermidis* with 1–7 was monitored using the microdilution assay. Growth inhibition in the microbial pathogens was quantified by monitoring the conversion of resazurin to the fluorescent resorufin product. The cytotoxicity of 1–7 in mammalian cells was assessed at 72 h post-incubation using a tetrazolium-based assay.

Not surprisingly, saturated C16 and C18 fatty acids (palmitic (4) and stearic acids (5), respectively) did not show any significant bioactivity against microbial pathogens or mammalian cells (Table 2). Only 3 was bioactive against planktonic *S. epidermidis* (MIC = 16 µg/mL), while 7 showed weak inhibition against planktonic *S. aureus* (MIC = 64 µg/mL). Four of the seven compounds (1, 2, 3, and 6) inhibited biofilm formation in *S. epidermidis*. Compound 3 demonstrated cytotoxicity in mammalian MDCK cells (Table 2).

A comparison of each structure to its bioactivity profile shows that decoration of the hydrophobic chain with various functional groups led to a variety of biological activities. For example, in the C16 fatty acids 2 and 4, the addition of an α,β -unsaturation in 4 led to cytotoxic activity against mammalian cells and modest inhibition of biofilm formation in *S. epidermidis* (Table 2). Comparing 2 and 3, the addition of one CH₂ group in the latter resulted in potent but non-selective activity against biofilm, planktonic *S. epidermidis*, and MDCK cells. Improved selectivity for biofilm inhibition was observed for compounds bearing an epoxide ring, as in 1 and 6. The selectivity index increased by

two- to four-fold with the introduction of the epoxide functionality. At the same time, **6** showed no antiproliferative action in mammalian cells.

Table 2. Minimum inhibitory concentration (MIC) and minimum biofilm inhibition concentration (MBIC) of **1–7** against staphylococcal pathogens ^a.

Compounds	MBIC (µg/mL) <i>S. epidermidis</i> RP62A (ATCC® 35984™)	MIC (µg/mL) <i>S. epidermidis</i> RP62A (ATCC® 35984™)	Selectivity Index (MIC _{Planktonic} /MBIC _{Biofilm})	MIC (µg/mL) <i>S. aureus</i> (ATCC® 6538™)	MIC (µg/mL) Methicillin- Resistant <i>S. aureus</i> (ATCC® 43,300™)	IC ₅₀ (µg/mL) MDCK NBL-2 (ATCC® CCL-34™)
1	32	128	~4	>128	>128	61.7
2	>128	>128	~1	>128	>128	33.0
3	16	16	~1	>128	>128	13.6
4	>128	>128	~1	>128	>128	>128
5	>128	>128	~1	>128	>128	>128
6	16	>128	>8	>128	>128	>128
7	>128	>128	~1	64.0	>128	>128
dispersin B	64	>>128	>>2	n/a	n/a	n/a
chloramphenicol	n/a	8.0	n/a	n/a	n/a	n/a
oxacillin	n/a	n/a	n/a	0.5	8	n/a

^a Data presented as MIC of two independent trials performed in quadruplicates. MIC defined as the lowest concentration with >98% growth inhibition. MBIC defined as the lowest concentration causing a >98% inhibition of biofilm formation. n/a = not applicable.

The potency and selectivity of the oxylipins are dictated by the addition of functional groups to the lipophilic chain. Having an electrophilic center improves the potency, while the nature of the functional groups tunes the selectivity. Electrophilic centers are a common feature among other compounds with biofilm-inhibitory activity such as in *cis*-2-decenoic acid [17,18], cinnamaldehyde [19], pentadecanal [20], 5-dodecanolide [21], parthenolide [22], and cembranoid alkaloid [23]. Pentadecanal, from the marine bacterium *Pseudoalteromonas haloplanktis* TAC125, is structurally related to the *Vibrio harveyi* quorum-sensing molecule tetradecanal [20]. Biofilm formation in methicillin-resistant *S. aureus* (MRSA) is restricted by 5-dodecanolide, which decreases the expression of the quorum-sensing genes *agrA* and *agrC*, consequently downregulating the expression of effector genes involved in biofilm formation [21]. The transcriptional effect of 5-dodecanolide is suggested to affect the early stages of biofilm formation by modulating the levels of adhesion proteins [21]. The anti-biofilm compounds **1–3** and **6** are similar to reactive electrophilic oxylipins which possess the qualities of being lipophilic and thiol-reactive. Thiol modification is assumed to represent a key mechanism in signal transduction [24]. These oxylipins chemically modify several proteins—particularly thioredoxins, which function in redox signaling and oxidative stress responses. A thioredoxin *trxHEp*, from the fish pathogen *Edwardsiella piscicida* was identified as contributing to the microorganism's adversity adaptation and its pathogenicity [25]. The deletion of *trxHEp* led to retarded bacterial biofilm growth [25]. Because the anti-biofilm activity is correlated with the presence of thiol-reactive groups, it is possible that **1–3** and **6** function similarly by covalently modifying bacterial proteins. Further work is required to test this hypothesis.

The existence of anti-biofilm compounds such as **1–3** from *T. turnerae* may have an ecological relevance to the shipworm host. Compounds **1–3** could be part of an arsenal of compounds, including the previously reported tartrolons and turnerbactin, for suppressing microbial growth within the caecum of the shipworm host, where lignocellulose is degraded and glucose is liberated. This would constitute a complex strategy involving the inhibition of biofilms with **1–3**, sequestration of iron by turnerbactin, and planktonic cell-killing by tartrolons in order to limit the proliferation of competing microbes [9,13]. Furthermore, the biotransformation of fatty acids to oxylipins by *T. turnerae* highlights an effective strategy to modulate the potency and selectivity of biological activity, starting with simple and abundant fatty acid precursors.

3. Materials and Methods

3.1. General Experimental Procedures

^1H , ^{13}C , and 2D NMR data were collected using a Varian Inova 500 MHz spectrometer equipped with a 3 mm NMR probe using residual solvent signals for referencing. Low-resolution ESIMS was done using a Shimadzu 8040 through direct injection in 50% MeOH:H₂O with 0.1% formic acid. High-resolution MS (HRMS) data were obtained using Waters Xevo G2 XS QTOF through direct infusion using 50% aqueous ACN with 0.1% formic acid. HPLC purification was done using a Shimadzu High-Performance Liquid Chromatograph (HPLC) equipped with binary pumps, fraction collector, and photodiode array detector (Shimadzu Kyoto, Japan). Fatty acids palmitic (4) and stearic acids (5) were sourced from Sigma-Aldrich (St. Louis, MO, USA). (\pm) *trans*-12,13-epoxy-octadecanoic acid (6) and 12(*Z*)-octadecenoic acid (7) were purchased from Larodan Fine Chemicals (Solna, Sweden).

3.2. Biological Material

T. turnerae strain 991H.S.0a.06 was obtained from the gill of *Lyrodus pedicellatus* collected in Panglao, Bohol, and identified through the amplification and sequencing of 16S rRNA genes using primers 27F (5'-AGAGTTTGATCMTGGCTCAG-3') and 1492R (5'-TACGGYTACCTTGTTACGACTT-3'). Sequences were submitted to GenBank with accession number MH379668.

3.3. Culturing and Extraction

T. turnerae 991H.S.0a.06 was grown for 7 days using a Shipworm Basal Medium broth (SBM) at 30 °C, 250 rpm. The SBM contained sucrose (5 g/L), NaCl (19.8 g/L), NH₄Cl (267.5 mg/L), MgCl₂·6H₂O (8.95 g/L), Na₂SO₄ (3.31 g/L), CaCl₂·2H₂O (1.25 g/L), NaHCO₃ (0.162 g/L), Na₂CO₃ (10 mg/L), KCl (0.552 mg/L), KBr (81 mg/L), H₃BO₃ (21.5 mg/L), SrCl₂·6H₂O (19.8 mg/L), KH₂PO₄ (3.82 mg/L), NaF (2.48 mg/L), Na₂MoO₄·2H₂O (2.5 mg/L), MnCl₂·4H₂O (1.8 mg/L), ZnSO₄·7H₂O (0.22 mg/L), CuSO₄·5H₂O (0.079 mg/L), Co(NO₃)₂·6H₂O (0.049 mg/L), Fe-EDTA complex (4.15 mg/L), and HEPES (4.76 g/L) adjusted to pH = 8.0. After the incubation period the broth was centrifuged, and the supernatant was extracted with HP20TM Diaion resin for 2 h. The filtered resin was washed with H₂O, 75% aqueous MeOH, and then eluted with 100% MeOH. The methanolic extract was dried under reduced pressure to yield the crude extract. This was subjected to solvent partitioning (3×) with EtOAc:H₂O (1:1 *v/v*). The bioactive organic extract was separated into four fractions using reversed phase C18 column chromatography with a step-gradient elution of MeOH in H₂O (40%, 60%, 80%, and 100%). The bioactive 100% MeOH C18 open-column fraction was further separated by size exclusion chromatography (Sephadex LH20) using MeOH as the eluting solvent. A total of 16 LH20 fractions were collected and subjected to silica thin-layer chromatography (TLC) using a 9:1 CH₂Cl₂:MeOH system as the developing solvent. Fractions were pooled based on similarity of the TLC profile to generate four fractions (Fractions 1–4). LH20 Fraction 2 was subjected using semipreparative reversed phase HPLC (Varian Polaris C-18 A-50, 250 × 10 mm, 5 μm; flowrate: 3.00 mL/min) in a linear gradient of MeOH:H₂O with 0.1% TFA as solvent system (60% MeOH:H₂O for 5 min, 60–100% MeOH:H₂O over 7.5 min, 100% MeOH for 5 min). Fractions were collected at 1 min intervals using a fraction collector. The bioactive fraction with *t*_R = 15.0 min, exhibiting antibiofilm activity, was further purified by semipreparative HPLC (Phenomenex Luna C18, 5 μm; 250 × 10 mm; flow rate, 3 mL/min) using a linear gradient of MeOH:H₂O with 0.1% TFA (75% MeOH:H₂O for 5 min, 75–95% MeOH:H₂O over 5 min, 100% MeOH for 15 min) to afford turneroic acid (1, *t*_R = 14.7 min, 1.4 mg). LH20 Fraction 4 was also fractionated using semipreparative RP-HPLC (Varian Polaris C-18 A-50, 250 × 10 mm, 5 μm; flowrate: 3 mL/min) with MeOH:H₂O with 0.1% TFA as solvent system (75–100% MeOH:H₂O in 25 min, 100% MeOH for 5 min) to afford 2 (3.2 mg, *t*_R = 13.5 min) and 3 (6.5 mg, *t*_R = 17.4 min).

Turneroic acid/11-hydroxy-12,13-epoxyoctadecanoic acid (1): white powder; UV (MeOH + 0.1% TFA) λ_{max} 230 nm; LC-ESIMS *m/z* 315.40 [M + H]⁺; HRESIMS *m/z* 337.2363 [M + Na]⁺ (calcd. for C₁₈H₃₄O₄Na 337.2355); ^1H NMR and ^{13}C NMR data, see Table 1.

3.4. Antimicrobial Microdilution Assay

The effects of 1–7 on planktonic *S. aureus* and methicillin-resistant *S. aureus* were assessed using a rezasurin-based method, as described in Lacerna et al. (2019) [26] and based on Sarker et al. (2007) [27]. In brief, *Staphylococcus aureus* (ATCC6538) and methicillin-resistant *S. aureus* (MRSA) (ATCC43300) were grown in Mueller Hinton broth (MHB) and treated with 1–7 after 24 h of inoculation. Compounds were tested using a two-fold dilution scheme from 0.25–128 µg/mL. After 24 h of incubation, 0.02% rezasurin (20 µL) was added to each well, and the fluorescence was measured at 530 nm excitation and 590 nm emission. MIC is the lowest concentration at which there was no reduction of the rezasurin dye, equivalent to 98% inhibition of microbial growth. Assays were done in two independent trials with four independent replicates.

3.5. Biofilm Inhibition Assay

The biofilm inhibition assay was done according to the method of Skogman et al. (2012) [28]. A glycerol stock of *Staphylococcus epidermidis* RP62A (ATCC35984) was revived on Congo red agar (CRA) plates and phenotypically characterized to form rough black colonies, suggesting its ability to produce the biofilm. A single colony from the CRA plate was transferred in 50 mL trypticasein soy broth supplemented with glucose (TSBg) and grown overnight at 35 °C, 150 rpm. The turbidity of the culture was adjusted to match the 0.5 McFarland standard (1×10^8 cells/mL) and diluted 100-fold prior to inoculation in a 96-well plate. These were treated with compounds 1, 4–7, in a series of two-fold dilution starting at 128 µg/mL to 0.250 µg/mL. Compounds 2–3 were tested using half-log dilutions starting at 500 µg/mL. TSBg served as the negative control, and positive controls were chloramphenicol (Sigma-Aldrich) for planktonic cells and dispersin B (Kane Biotech) for biofilms. Dispersin B is a 40 kDa glycoside hydrolase which dissolves mature bacterial biofilms [29]. The plates were incubated for 20 h at 37 °C without shaking to facilitate biofilm formation. At the end of the incubation period, the planktonic suspension was transferred to another 96-well plate to assess cell viability. A 20 µL-aliquot of 0.02% rezasurin was added to each well and incubated for 30 min at 37 °C, 150 rpm. Fluorescence was measured using a 530 nm excitation filter and a 590 nm emission filter. To quantify the formed biofilm, 100 µL-aliquot of wheat germ agglutinin Alexa Fluor 488 (WGA488) probe (50 µg/mL) was added to each well of the original plate and incubated in the dark at 4 °C for 5 h. At the end of incubation, the plate was washed with sterile PBS (3×) and air-dried at room temperature to remove the unbound WGA488 probe. Bound stain to the biofilm was dissolved in 33% glacial acetic acid and quantified by fluorescence measurement at 485 nm/420 nm excitation filters, and 528 nm/520 nm emission filters. Minimum biofilm inhibitory concentration (MBIC) is the lowest concentration that resulted in 98% inhibition of biofilm formation. This was done in two independent trials with four independent replicates.

3.6. Mammalian Antiproliferative Assay

The mammalian antiproliferative assay was done according to Lacerna et al. (2019) and modified from the method of Mossman (1983) [30]. MDCK NBL-2 (ATCC CCL-34) cells were treated with 1–7 at half-log dilution starting at 500 µg/mL. At 72 h post-incubation, the cells were treated with MTT and the absorbance at 570 nm was read. The IC₅₀ was calculated using GraphPad Prism 5 based on a 4-point sigmoidal non-linear regression analysis of cell viability vs. log concentration of the inhibitor. The assay was done in two independent trials with four independent replicates.

Supplementary Materials: The following are available online at <http://www.mdpi.com/1660-3397/18/12/656/s1>. Figures S1–S6: HRMS, ¹H NMR, COSY, HSQC, HMBC, and TOCSY spectra of turneroic acid (1); Figures S7 and S8: LC-ESI-MS of 2 and 3; Figures S9 and S10: MS/MS spectra of 2 and 3; Figures S11 and S12: ¹H NMR spectra of 2 and 3; Figures S13–S15: Concentration-dependent curves of 1–7 against *S. epidermidis* biofilm formation and planktonic *S. epidermidis* cells; Figure S16: Concentration-dependent curve of oxacillin against *S. aureus* and methicillin-resistant *S. aureus*.

Author Contributions: Conceptualization, N.M.I.II, J.M.R., L.A.S.-R., and G.P.C.; methodology, N.M.I.II, C.V.R., J.M.R., M.R.D.P., J.O.T., and L.A.S.-R.; writing—original draft preparation, N.M.I.II, L.A.S.-R., and G.P.C.; review and editing— N.M.I.II, B.W.M., M.G.H., E.W.S., L.A.S.-R., and G.P.C.; funding acquisition, M.G.H. and G.P.C. All authors have read and agreed to the published version of the manuscript.

Funding: Research reported in this publication was supported by the Fogarty International Center of the National Institutes of Health under Award Number U19TW008163. The content is solely the responsibility of the authors and does not necessarily represent the official views of the National Institutes of Health. The work was completed under supervision of the Department of Agriculture-Bureau of Fisheries and Aquatic Resources, Philippines (DA-BFAR) in compliance with all required legal instruments and regulatory issuances covering the conduct of the research. This work is part of the MSc and BSc thesis of N. Lacerna and C. Ramones, respectively.

Conflicts of Interest: The authors declare no conflict of interest.

References

1. Donlan, R.M. Role of Biofilms in Antimicrobial Resistance. *ASAIO J.* **2000**, *46*, S47–S52. [[CrossRef](#)] [[PubMed](#)]
2. Roy, R.; Tiwari, M.; Donelli, G.; Tiwari, V. Strategies for combating bacterial biofilms: A focus on anti-biofilm agents and their mechanisms of action. *Virulence* **2018**, *9*, 522–554. [[CrossRef](#)] [[PubMed](#)]
3. Santos, A.L.S.D.; Galdino, A.C.M.; De Mello, T.P.; Ramos, L.D.S.; Branquinha, M.H.; Bolognese, A.M.; Neto, J.C.; Roudbary, M. What are the advantages of living in a community? A microbial biofilm perspective! *Memórias do Instituto Oswaldo Cruz* **2018**, *113*, e180212. [[CrossRef](#)] [[PubMed](#)]
4. Otto, M. Staphylococcal Biofilms. *Curr. Top. Microbiol. Immunol.* **2008**, *322*, 207–228.
5. Otto, M. Staphylococcus epidermidis—The “accidental” pathogen. *Nat. Rev. Microbiol.* **2009**, *7*, 555–567. [[CrossRef](#)]
6. Rossiter, S.E.; Fletcher, M.H.; Wuest, W.M. Natural products as platforms to overcome antibiotic resistance. *Chem. Rev.* **2017**, *117*, 12415–12474. [[CrossRef](#)]
7. Schmidt, E.W. Trading molecules and tracking targets in symbiotic interactions. *Nat. Chem. Biol.* **2008**, *4*, 466–473. [[CrossRef](#)]
8. Piel, J. Metabolites from symbiotic bacteria. *Nat. Prod. Rep.* **2009**, *26*, 338–362. [[CrossRef](#)]
9. Han, A.W.; Sandy, M.; Fishman, B.; Trindade-Silva, A.E.; Soares, C.A.G.; Distel, D.L.; Butler, A.; Haygood, M.G. Turnerbactin, a Novel Triscatecholate Siderophore from the Shipworm Endosymbiont *Teredinibacter turnerae* T7901. *PLoS ONE* **2013**, *8*, e76151. [[CrossRef](#)]
10. Distel, D.L.; Altamia, M.A.; Lin, Z.; Shipway, J.R.; Han, A.; Forteza, I.; Antemano, R.; Limbaco, M.G.J.P.; Tebo, A.G.; Dechavez, R.; et al. Discovery of chemoautotrophic symbiosis in the giant shipworm *Kuphus polythalamia* (Bivalvia: Teredinidae) extends wooden-steps theory. *Proc. Natl. Acad. Sci. USA* **2017**, *114*, E3652–E3658. [[CrossRef](#)]
11. Waterbury, J.B.; Calloway, C.B.; Turner, R.D. A Cellulolytic Nitrogen-Fixing Bacterium Cultured from the Gland of *Deshayes* in Shipworms (Bivalvia: Teredinidae). *Science* **1983**, *221*, 1401–1403. [[CrossRef](#)] [[PubMed](#)]
12. Yang, J.C.; Madupu, R.; Durkin, A.S.; Ekborg, N.A.; Pedamallu, C.S.; Hostetler, J.B.; Radune, D.; Toms, B.S.; Henrissat, B.; Coutinho, P.M.; et al. The Complete Genome of *Teredinibacter turnerae* T7901: An Intracellular Endosymbiont of Marine Wood-Boring Bivalves (Shipworms). *PLoS ONE* **2009**, *4*, e6085. [[CrossRef](#)] [[PubMed](#)]
13. Elshahawi, S.I.; Trindade-Silva, A.E.; Hanora, A.; Han, A.W.; Flores, M.S.; Vizzoni, V.; Schrago, C.G.; Soares, C.A.G.; Concepcion, G.P.; Distel, D.L.; et al. Boronated tartrolon antibiotic produced by symbiotic cellulose-degrading bacteria in shipworm gills. *Proc. Natl. Acad. Sci. USA* **2013**, *110*, E295–E304. [[CrossRef](#)] [[PubMed](#)]
14. Yuan, Z.-X.; Majchrzak-Hong, S.; Keyes, G.S.; Iadarola, M.J.; Mannes, A.J.; Ramsden, C.E. Lipidomic profiling of targeted oxylipins with ultra-performance liquid chromatography-tandem mass spectrometry. *Anal. Bioanal. Chem.* **2018**, *410*, 6009–6029. [[CrossRef](#)]
15. Hung, T.D.; Hye, J.L.; Eun, S.Y.; Shinde, P.B.; Yoon, M.L.; Hong, J.; Kim, D.K.; Jung, J.H. Anti-inflammatory constituents of the Red Alga *Gracilaria verrucosa* and their synthetic analogues. *J. Nat. Prod.* **2008**, *71*, 232–240.
16. Abou-ElWafa, G.S.E.; Shaaban, M.; Shaaban, K.A.; El-Naggar, M.E.E.; Laatsch, H. Three New Unsaturated Fatty Acids from the Marine Green Alga *Ulva fasciata* Delile. *Zeitschrift für Naturforschung B* **2009**, *64*, 1199–1207. [[CrossRef](#)]

17. Davies, D.; Marques, C. A fatty acid messenger is responsible for inducing dispersion in microbial biofilms. *J. Bacteriol.* **2009**, *191*, 1393–1403. [[CrossRef](#)]
18. Marques, C.; Morozoz, A.; Planzos, P.; Zelaya, H. The fatty acid signaling molecule cis-2-decenoic acid increases metabolic activity and reverts persister cells to an antimicrobial-susceptible state. *Appl. Environ. Microbiol.* **2014**, *80*, 6976–6991. [[CrossRef](#)]
19. Topa, S.H.; Subramoni, S.; Palombo, E.A.; Kingshott, P.; Rice, S.A.; Blackall, L.L. Cinnamaldehyde disrupts biofilm formation and swarming motility of *Pseudomonas aeruginosa*. *Microbiology* **2018**, *164*, 1087–1097. [[CrossRef](#)]
20. Casillo, A.; Papa, R.; Ricciardelli, A.; Sannino, F.; Ziaco, M.; Tilotta, M.; Selan, L.; Marino, G.; Corsaro, M.M.; Tutino, M.L.; et al. Anti-Biofilm Activity of a Long-Chain Fatty Aldehyde from Antarctic *Pseudoalteromonas haloplanktis* TAC125 against *Staphylococcus epidermidis* Biofilm. *Front. Cell. Infect. Microbiol.* **2017**, *7*, 46. [[CrossRef](#)]
21. Valliammai, A.; Sethupathy, S.; Priya, A.; Selvaraj, A.; Bhaskar, J.P.; Krishnan, V.; Pandian, S.K. 5-Dodecanolide interferes with biofilm formation and reduces the virulence of Methicillin-resistant *Staphylococcus aureus* (MRSA) through up regulation of agr system. *Sci. Rep.* **2019**, *9*, 1–16. [[CrossRef](#)] [[PubMed](#)]
22. Romero, D.; Sanabria-Valentín, E.; Vlamakis, H.; Kolter, R. Biofilm Inhibitors that Target Amyloid Proteins. *Chem. Biol.* **2013**, *20*, 102–110. [[CrossRef](#)] [[PubMed](#)]
23. Camacho, E.T.; Castellanos, L.; Arévalo-Ferro, C.; Duque, C. Disruption in Quorum-Sensing Systems and Bacterial Biofilm Inhibition by Cembranoid Diterpenes Isolated from the Octocoral *Eunicea knighti*. *J. Nat. Prod.* **2012**, *75*, 1637–1642. [[CrossRef](#)]
24. Mueller, M.J.; Berger, S. Reactive electrophilic oxylipins: Pattern recognition and signalling. *Phytochem.* **2009**, *70*, 1511–1521. [[CrossRef](#)]
25. Wang, B.-Y.; Huang, H.-Q.; Li, S.; Tang, P.; Dai, H.; Xian, J.-A.; Sun, D.-M.; Hu, Y. Thioredoxin H (TrxH) contributes to adversity adaptation and pathogenicity of *Edwardsiella piscicida*. *Veter. Res.* **2019**, *50*, 26. [[CrossRef](#)] [[PubMed](#)]
26. Lacerna, I.N.M.; Miller, B.W.; Lim, A.L.; Tun, J.O.; Robes, J.M.D.; Cleofas, M.J.B.; Lin, Z.; Salvador-Reyes, L.A.; Haygood, M.G.; Schmidt, E.W.; et al. Mindapyrroles A–C, Pyoluteorin Analogues from a Shipworm-Associated Bacterium. *J. Nat. Prod.* **2019**, *82*, 1024–1028. [[CrossRef](#)]
27. Sarker, S.D.; Nahar, L.; Kumarasamy, Y. Microtitre plate based antibacterial assay incorporatin resazurin as an indicator of cell growth, and its applications in the in vitro antibacterial screening of phytochemicals. *Methods* **2007**, *42*, 321–324. [[CrossRef](#)]
28. Skogman, M.E.; Vuorela, P.M.; Fallarero, A. Combining biofilm matrix measurements with biomass and viability assays in susceptibility assessments of antimicrobials against *Staphylococcus aureus* biofilms. *J. Antibiot.* **2012**, *65*, 453–459. [[CrossRef](#)]
29. Yan, Z.; Huang, M.; Melander, C.; Kjellerup, B.V. Dispersal and inhibition of biofilms associated with infections. *J. App. Microbiol.* **2020**, *128*, 1279–1288. [[CrossRef](#)]
30. Mosmann, T. Rapid colorimetric assay for cellular growth and survival: Application to proliferation and cytotoxicity assays. *J. Immunol. Methods* **1983**, *65*, 55–63. [[CrossRef](#)]

Publisher’s Note: MDPI stays neutral with regard to jurisdictional claims in published maps and institutional affiliations.



© 2020 by the authors. Licensee MDPI, Basel, Switzerland. This article is an open access article distributed under the terms and conditions of the Creative Commons Attribution (CC BY) license (<http://creativecommons.org/licenses/by/4.0/>).